Automotive Science and Engineering, Vol. 15, No. 4, (2025), 4871-4886

Iran University of Science and Technology

Automotive Science and Engineering

Journal Homepage: ase.iust.ac.ir

ISSN: 2008-9899

Durability-Driven Energy Management for Fuel Cell Hybrid EVs: Multi-Scenario Optimization Across Different Traffic and Driving Cycles

Morteza Montazeri-Gh [1*], Mohammad Amin Zakizadeh[2], Afshin Mostashiri [3]

Systems simulation and control laboratory, School of mechanical engineering, Iran university of science and technology, Tehran 16846-13114, Iran

1* Professor, Mechanical Engineering, Iran University of Science and Technology, Tehran, Iran.

2 M.Sc. Student, Mechanical Engineering, Iran University of Science and Technology, Tehran, Iran.

3 Phd. Student, Mechanical Engineering, Iran University of Science and Technology, Tehran, Iran.

ARTICLE INFO

Article history:

Received : 13 Mar 2025

Accepted: 9 Oct 2025

Published: 4 Nov 2025

Keywords:

Fuel cell hybrid vehicles

Optimization

fuzzy energy management

Durability

Trafic diving cycle

A B S T R A C T

The rising demand for sustainable transportation has intensified research on Fuel Cell Hybrid Electric Vehicles (FCHEVs). Integrating fuel cells with lithium-ion batteries provides a pathway to enhance energy efficiency and driving performance, but ensuring the durability of both components under real operating conditions remains a critical challenge. This work proposes an integrated framework to improve FCHEV performance and lifetime through combined modeling, degradation analysis, and optimized energy management. Dynamic vehicle simulations were conducted using the ADVISOR platform under both the Urban Dynamometer Driving Schedule (UDDS) and a real-world cycle based on Tehran traffic data. Degradation models were implemented to capture platinum dissolution in the Proton Exchange Membrane Fuel Cell (PEMFC) and capacity loss in the lithium-ion battery, incorporating the effects of state of charge, temperature, and current rate. An energy management strategy was developed using a Fuzzy Logic Controller (FLC) for fuel cell–battery power distribution, which was further refined with a Genetic Algorithm (GA). The optimization objectives included reducing hydrogen consumption and extending component lifetimes. The GA-optimized FLC extended PEMFC lifetime by 50.6% Tehran and 12.9% UDDS and reduced battery capacity fade by 10% and 4.9%, respectively. While *direct* hydrogen consumption increased in Tehran due to more aggressive regenerative-energy routing to the battery, the Equivalent Fuel Consumption (EFC) decreased from 971.32 → 937.21 g/100 km (Tehran) and 794.41 → 782.24 g/100 km (UDDS), reflecting a net efficiency gain once SOC restoration is accounted for.

1. Introduction

With the rising demand for clean and efficient transportation, fuel cell hybrid electric vehicles (FCHEVs) integrated with battery energy storage systems have become a promising solution. These vehicles aim to reduce fuel consumption and enhance performance, thereby playing a vital role in decreasing reliance on fossil fuels. A significant challenge in FCHEV design and optimization lies in extending the lifespan of the fuel cell and the battery, which are heavily influenced by driving patterns and traffic conditions.

Recent research has concentrated on optimizing power distribution and vehicle design. For example, genetic algorithms have effectively optimized power management strategies, resulting in prolonged battery and

*Corresponding Author
Email Address: montazeri@iust.ac.ir
https://doi.org/10.22068/ase.2025.719

"*Automotive Science and Engineering*" is licensed under a Creative Commons Attribution-Noncommercial 4.0 International License.

[Downloaded from ahc.iust.ac.ir on 2026-06-05]

[DOI: 10.22068/ase.2025.719]

fuel cell life, reduced hydrogen consumption, and lower overall ownership costs[1]. Investigations into battery degradation demonstrate that refined energy management strategies can significantly improve vehicle performance while minimizing costs[2]. Due to the high expense and limited durability of fuel cells and batteries, advanced energy management is essential to extend their operational life and reduce costs. Moreover, online optimization techniques have been developed to mitigate degradation under real-world driving scenarios[3]. Predictive models for battery lifespan and energy loss minimization have been proposed, contributing to fuel savings and improved battery longevity[4]. Artificial intelligence approaches, such as self-discharge (SD) based models, have enhanced the accuracy of battery performance and remaining useful life predictions[5]. Additionally, hybrid control methods combining fuzzy logic and switching techniques have been explored to bolster fuel cell durability and optimize fuel consumption in FCHEVs[6]. A prior work formulated the joint optimization of power management and component sizing in plug-in hybrid fuel cell/lithium-ion battery vehicles as a constrained multi-objective problem (MOP) [7], seeking to minimize fuel use and cost subject to performance limits. To solve this, a particle swarm optimization algorithm based on Pareto dominance (PMOPSO) was developed, successfully generating a set of optimal design and energy management solutions.

As transportation depends heavily on fossil fuels, energy management in PEMFC based plug-in hybrid sedans has gained prominence[8]. A two-stage control strategy was introduced to reduce hydrogen consumption and safeguard fuel cell health, achieving a balanced trade-off between fuel economy and durability, as validated through Matlab/Simulink simulations. Enhancing lithium-ion battery longevity is fundamental to sustainable electric mobility. Degradation processes involve interdependent electrochemical, thermal, and mechanical mechanisms influenced by material composition, operational parameters, and system architecture. Load reduction strategies are practical to prolong battery life, though optimal implementation and effects remain under investigation. Reviews categorize these strategies into dynamic and static methods[9]. Estimating battery capacity loss and remaining life online, particularly under real driving conditions, remains challenging but crucial for effective vehicle energy management. A method employing genetic algorithms for component sizing based on empirical driving data was applied to a hybrid vehicle, demonstrating practical capacity loss estimation and a clear correlation between battery degradation and driving conditions[10].

In addition to control-oriented approaches, the component sizing of hybrid energy-storage systems plays a crucial role in determining overall durability and efficiency. The ratio between fuel-cell power and battery capacity directly affects the average current density, temperature rise, and depth of discharge—parameters that accelerate degradation if not properly balanced. Studies on optimum sizing and energy-management co-design[11], have shown that carefully selected power-energy ratios can substantially extend battery life while maintaining high system efficiency. Building on these insights, the present research concentrates on the control dimension of durability—developing a GA-optimized fuzzy logic controller for a fixed but realistic FC/battery configuration—as a foundation for future integration with size-optimization frameworks.

Despite these advances, few studies integrate battery degradation modeling with energy

[Downloaded from ahc.iust.ac.ir on 2026-06-05]

[DOI: 10.22068/ase.2025.719]

management under real-world traffic conditions in a way that is both computationally efficient and practically applicable. To address this gap, the present study proposes a durability-driven energy management strategy that jointly considers fuel cell aging and battery degradation. By integrating physical degradation models into a fuzzy-logic-based control system, and further optimizing the controller with a genetic algorithm, the approach aims to extend system lifetime while also reducing hydrogen consumption. The proposed framework is validated through simulations on two driving cycles: the standardized UDDS cycle and a real-world traffic cycle developed for Tehran. The results demonstrate measurable gains in durability, energy efficiency, and stability of state of charge, suggesting that this method provides a practical pathway for improving the reliability of FCHEVs in real-world use.

2. Analysis of Fuel Cell Hybrid Electric Vehicle Performance Based on Driving Cycles

A driving cycle is a time-based speed profile that simulates typical driving behavior in a specific city or region. It is shaped by the road network, traffic conditions, driving culture, and geographic characteristics. Driving cycles are fundamental in assessing vehicle performance, with particular importance for modeling and managing energy in fuel-cell hybrid electric vehicles To really understand and improve energy systems, it's important to test them under the right driving conditions. In this study, among the driving cycles examined, the UDDS is depicted in Figure 1, which reflects common city driving, and (Figure 2) the Tehran traffic cycle, built from real traffic data and local driving habits. Looking at how fuel-cell hybrid cars perform in both cases gives a clearer picture of their energy use and points to better ways of making them more efficient.

Using the ADVISOR environment, a dynamic model of the fuel cell hybrid vehicle was formulated. To ensure the results reflect a range of driving conditions, several cycles were included in the simulations: UDDS, the European cycle, and a Tehran-specific cycle based on local traffic data. The main technical details of the vehicle are listed in Table 1, covering the battery pack, fuel cell stack, electric motor, and transmission. All of these parts were brought together in the simulation so their interactions could be studied. In this setup, the fuel cell works as the main power source, the battery stores extra energy, and the motor turns that energy into movement. The electronic control unit (ECU) keeps everything coordinated to get the best performance out of the system. Figure 3 shows how these subsystems work together and highlights the way they contribute to improving the vehicle's efficiency.

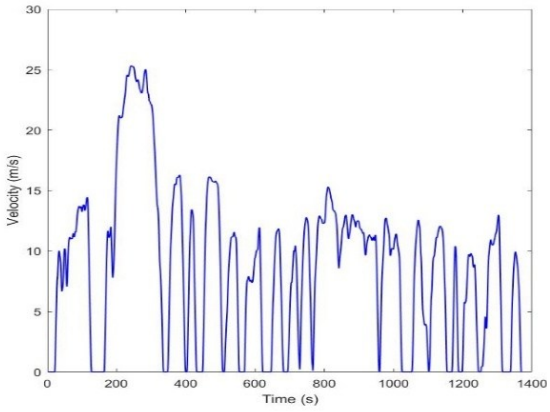

Figure 1: UDDS drive cycle

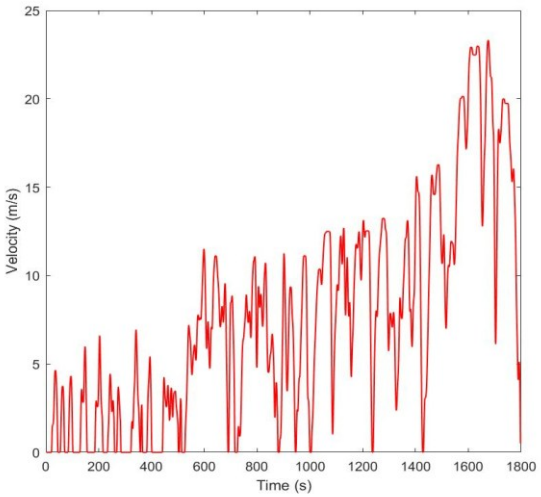

Figure 2: TEHRAN drive cycle

[Downloaded from ahc.iust.ac.ir on 2026-06-05]

[DOI: 10.22068/ase.2025.719]

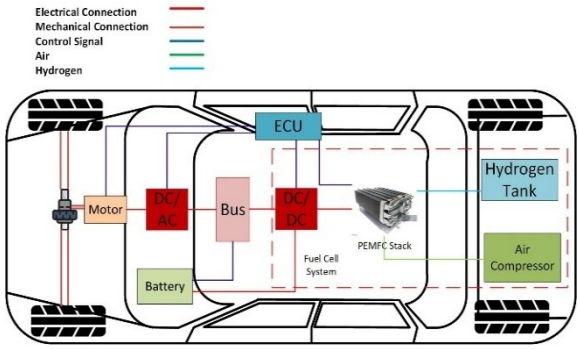

Figure 3: Basic structure of a fuel cell hybrid vehicle

Table 1: Fuel cell hybrid vehicle specifications

Components	Quality	Value	Unite
Vehicle specifications	Drag coefficient (C_D)	0.318	--
	Front view area (A_f)	2.1	m^2
	Effect coefficient of rotating objects (δ)	1.078	-
	vehicle Weight	1531	Kg
Battery[12]	Nominal capacity	37	Ah
	Voltage	350	V
Fuel cell	Maximum power	70	KW
	Active area	320	cm^2
Motor	Maximum power	75	KW
	Maximum speed	6000	rpm
	Maximum torque	280	Nm

3. Modeling of electrochemical surface degradation (ECSA) and voltage drop in fuel cells

Electrochemical surface area degradation and voltage loss are two major issues that strongly affect both the performance and lifespan of fuel cells. ECSA degradation is mainly caused by the dissolution of platinum, which is a key factor in the durability and efficiency of fuel cell catalysts. In this study [13,14], the platinum dissolution model proposed by Robin, Gerard, and their team is used. The model explains the process in three steps: first, platinum atoms detach from the crystal lattice; second, these atoms undergo oxidation; and finally, the oxidized atoms are removed from the catalyst surface.

The overall energy of this process is obtained by adding together the energy contributions from each stage, calculated through density functional theory (DFT). The free energy of oxidation ($\Delta G_{elec} = -2\alpha F \Delta\chi$) is derived from transition state theory (TST) and reflects the influence of the local electrochemical potential. The free energy of desorption (ΔG_{des}) is determined using an empirical correlation. Finally, the kinetic rate of platinum dissolution (v_{diss}) is expressed by an equation that describes how the radius of platinum nanoparticles changes with time.

This comprehensive modeling approach provides a mechanistic understanding of catalyst degradation phenomena, offering valuable insights for enhancing the durability and performance of fuel cell systems.

$$v_{diss} = ke^{-\frac{\Delta G}{RT}} = ke^{\frac{(-\Delta G_S + 2\alpha F\Delta\chi + \beta E_{Gt})}{RT}} \quad (1)$$

$$\frac{dr_{pt}}{dt} = -v_{diss}\frac{M_{pt}}{\rho_{pt}} \quad (2)$$

In fuel cells, voltage loss mainly arises from the oxidation of the platinum catalyst. In this reaction, platinum combines with oxygen to form platinum oxide (PtO), which reduces the catalyst's activity and, in turn, negatively affects the overall performance of the system. A linear model is developed to accurately predict cell voltage degradation over time, correlating the platinum oxide voltage (V_{pto}) with the catalyst's aging duration [15].

[Downloaded from ahc.iust.ac.ir on 2026-06-05]

[DOI: 10.22068/ase.2025.719]

$$V_{pto}(t) = V_{pto,0} + V_{pto,1}t \quad (3)$$

An exponential model is also used to estimate the reduction in crossover current density (i_{loss}) [16]:

$$i_{\text{loss}}(t) = i_{\text{loss},o} \exp\left(i_{\text{loss},1}t\right) \quad (4)$$

An exponential model is used to describe the changes in resistance over time [17]:

$$R(t) = R_0\, exp(R_1 t) \quad (5)$$

Additionally, the concentration decreases exponentially and is described by two parameters related to aging [18]:

$$m_t = m_o\, exp(m_1 t) \quad (6)$$

$$n_t = n_o\, exp(n_1 t) \quad (7)$$

The estimation of reversible voltage is also performed using the following equation [19]:

$$E_{rev} = 1.229 - 0.85 * 10^{-3}(T - 298.15) + 4.309 * 10^{-3} T \left[ln(P_{H2}) + \frac{1}{2} ln(P_{o2})\right] \quad (8)$$

Finally, the total fuel cell voltage is calculated by combining the above relationships as follows:

$$V = E_{\text{rev}} - \left(V_{\text{PtO,o}} + V_{PtO,1}t\right) - \frac{RT}{2\alpha_a F} ln\left(\frac{i(t)+i_{\text{loss},o}\exp(i_{\text{loss},1}t)}{i_{o,a}}\right) - \frac{RT}{4\alpha_c F} ln\left(\frac{i(t)+i_{\text{loss},o} exp\,(i_{\text{loss},1}t)}{i_{o,c}}\right) - i(t)(R_0 \cdot ex\,p(R_1 t) - m_0 \cdot ex\,p(m_1 t)[exp(i(t) \cdot n_0 \cdot exp(n_1 t)) - 1] \quad (9)$$

This equation expresses how aging parameters affect the decline in fuel cell voltage and efficiency. The model incorporates seven time-dependent aging parameters (V_{pto} ،α_a ،i_{loss} ، α_c ،R ، n ، m), which progressively diminish during operation, reflecting catalyst degradation, membrane resistance growth, and electrochemical surface area loss. Two fundamental constants (F, R) remain invariant, while four adjustable parameters (T E_{rev} , $i_{o,c}$, and $i_{o,a}$) enable operational optimization to mitigate performance decay. The charge transfer coefficient (α) requires careful calibration, as its value critically affects activation losses and catalyst kinetics [17]. For implementation guidance, consult methodologies combining empirical aging models with parameter identification techniques, such as polarization curve fitting or adaptive Kalman filters.

Figure 4 makes it clear that as current density increases, the fuel cell's voltage steadily drops. This happens because of resistance inside the cell and limits in the reaction itself. Over the first 300 hours, the drop becomes more noticeable and lines up with a reduction in Electrochemical Surface Area. As the ECSA shrinks, the electrode has fewer active sites, which means the catalyst works less effectively. At first, higher current density boosts output power, but after reaching a peak, the losses take over and power starts to fall. With time, as the ECSA keeps declining, the maximum power the cell can produce also goes down. By 300 hours, when the ECSA falls to 0.7766, the power output at higher current densities drops sharply, showing just how much the catalyst has degraded and how efficiency suffers as a result.

3.1. Environmental Effects and Parameter Drift

Environmental and aging effects were considered in the modeling phase through parameterized maps representing temperature-dependent and time-dependent degradation of both PEMFC and Li-ion battery. The PEMFC model includes gradual voltage reduction and resistance increase over time, while the battery model captures capacity fade and power loss with depth of discharge. These maps emulate realistic drift behavior under varying operating conditions. However, the control system assumes these effects are known and bounded, without applying adaptive rule updates during operation. Although the present fuzzy logic controller (FLC) assumes nominal operating conditions, temperature and ambient variations can gradually shift component characteristics such as stack voltage efficiency, battery internal resistance, and available power limits. To capture these dependencies, the degradation sub-models used in this study include temperature-dependent coefficients for both PEMFC voltage decay and Li-

[Downloaded from ahc.iust.ac.ir on 2026-06-05]

[DOI: 10.22068/ase.2025.719]

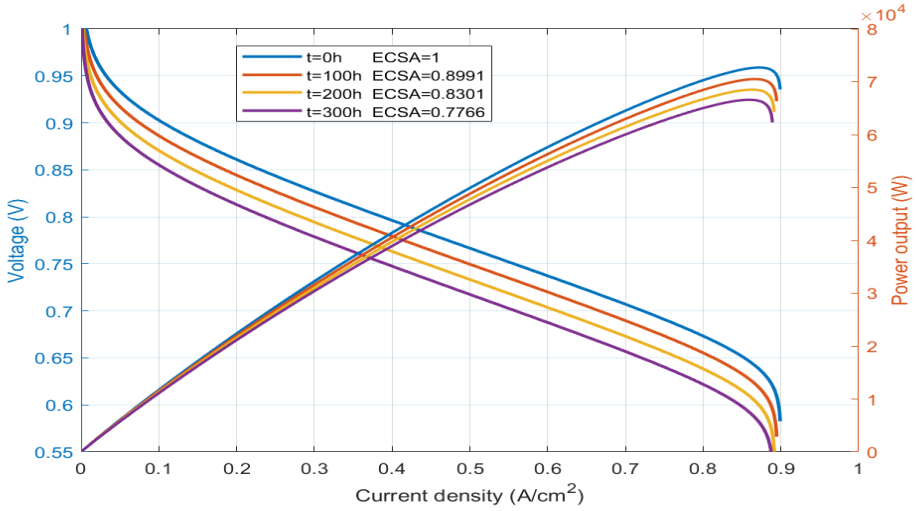

Figure 4: Polarization curve and relative power curve under certain time and ECSA

ion capacity fade. However, the controller itself currently does not update its rule base online. In future work, adaptive extensions could be implemented by incorporating state-of-power (SOP) or state-of-health (SOH) observers to track parameter drift in real time and by scheduling FLC membership functions according to cell temperature and estimated SOP. A hybrid Model Predictive Control (MPC)–FLC structure, as demonstrated in [20], could further improve constraint handling and responsiveness under fluctuating thermal or traffic conditions.

4. Cycle Aging Prediction Model for Lithium-Ion Batteries

In this study, the battery is represented by an equivalent electrical circuit, which allows its dynamic behavior and operating characteristics to be captured more accurately. The model takes the battery's power demand as an input, estimated from the SOC and internal resistance. With this setup, battery performance can be predicted more reliably across different conditions. In many laboratory studies, battery cycle life is tested using standardized or synthetic profiles. While useful, these profiles don't always match how batteries are actually used, so the results may not fully reflect real-world behavior. For example, the aging model in reference [21] is based on experimental data but does not account for the role of SOC. This is important because SOC strongly influences both performance and lifetime. Other factors, such as depth of discharge (DOD) and charging patterns, also shape how quickly capacity fades and how long the battery can last.

How a battery ages in practice depends on more than just its design—it is also strongly influenced by factors such as temperature, charging rate, and everyday usage patterns. If a model is based only on controlled laboratory tests and leaves out the effect of state of charge, it cannot fully reflect real operating conditions. To make predictions more meaningful, models need to capture the influence of SOC together with these environmental and operational factors. With this integration, aging models provide a truer picture of battery behavior and allow for more reliable assessments of long-term performance.

Reference [22] employed a square wave current profile to describe capacity degradation. A battery aging model was developed for systems similar to those in fuel cell hybrid electric vehicles, specifically targeting charging scenarios at low SOC conditions. The model incorporated the temperature dependence of capacity fade using the Arrhenius equation; however, its validation was limited, as it did not cover a broad range of temperatures. In the referenced[23] study, aging tests were performed using a standard load profile that systematically varied temperature, DOD, and current rates (C-rates) to analyze their individual effects on capacity fade. While the analysis provided insights into how each parameter influences battery degradation, it did not yield a unified aging

[Downloaded from ahc.iust.ac.ir on 2026-06-05]

[DOI: 10.22068/ase.2025.719]

model that simultaneously accounts for the combined effects of all these factors. As a result, the model lacks the comprehensiveness needed to accurately predict battery aging under real-world FCHEV operating conditions, where multiple stressors interact dynamically.

This research uses a damage accumulation model calibrated with historical battery data from a hybrid electric vehicle (HEV) to predict battery cycle life. This model incorporates dependencies on SOC, temperature, and current rate. The damage accumulation models proposed in references [24,25],[21] describe the effects of aging factors such as current rate (Ic), temperature (q), and SOC based on accumulated damage during operational conditions expressed in ampere-hours or total cycle count.

Q_{loss}, representing normalized capacity loss, is utilized here to assess battery degradation dynamics.

$$Q_{loss}(p,A) = \frac{Q_{batt}(0) - Q_{batt}(p,A)}{Q_{batt}(0)} \quad (10)$$

The aging factor vector p (comprising Ic, Tc, SOC) defines the operating conditions, where $Q_{batt}(0)$ and $Q_{batt}(p,A)$ symbolize the initial and degraded capacities, respectively. The capacity degradation model is expressed as:

$$Q_{loss}(p,Ah) = \sigma_{func}(p).A^{z} \quad (11)$$

The term $\sigma_{func}(p)$ denotes a nonlinear mapping of the aging factors (Ic, Tc, SOC), formulated as follows:

$$\sigma_{func}(p) = (\alpha.SOC + \beta).exp\left(\frac{-E_a + \eta.I_c}{R.(273.15 + \theta)}\right) \quad (12)$$

Here, α and β define the dependence on SOC, η models the dependence on Ic, the activation energy (Ea) has a value of 31,500 [J/mol], θ represents the battery temperature [°C] , and R is the universal gas constant.

This study proposes a two-step approach to identify the parameters of the proposed capacity degradation model.

Step One: This stage involves identifying the parameters z and σ_{func} from experimental data. For further model refinement, the average value of z is taken as 0.57.

Step Two: In this stage, the parameter η is set to 152.2. The severity factor function parameters, specifically α and β, are identified based on the experimental data presented in Table 2.

These steps are designed to enhance the accuracy of the capacity degradation model and align it more closely with experimental observations. The ultimate goal is to improve the predictive capability of the battery's performance under real-world operating conditions.

Table 2: Optimal values of α and β [26]

	$\alpha(SOC)$	$\beta(SOC)$
SOC < 45%	2896.6	7411.2
SOC≥ 45%	2694.5	6022.2

Since a 20% capacity loss is commonly considered the end of life (EOL) for batteries in automotive applications, a value of Q_{loss} = 20% is assigned in equation (11). Then, the total discharged capacity $A_{\text{total}}\,(I_c, T_c)$ and the corresponding number of cycles until EOL can be calculated as follows:

$$A_{\text{total}}\,(I_c, T_c) = \left[\frac{20}{\sigma_{\text{func}}(\text{p})}\right]^{\frac{1}{z}} \quad (13)$$

$$N(I_c, T_c) = \frac{A_{\text{total}}\,(I_c, T_c)}{C_{\text{bat}}} \quad (14)$$

Using these equations, the cumulative discharged capacity and cycle count to end-of-life can be quantified. The residual battery capacity is subsequently derived as:

$$Q(t) = Q(t_0) - \frac{\int_{t_0}^{t} |I(\tau)| d\tau}{2\times 3600 N(I_c, T_c) C_{bat}} \quad (15)$$

The degradation rate of battery capacity is obtained by differentiating equation (16):

$$\dot{Q}(t) = -\frac{|I(t)|}{2N(I_c, T_c) C_{bat}} \quad (16)$$

[Downloaded from ahc.iust.ac.ir on 2026-06-05]

[DOI: 10.22068/ase.2025.719]

From equation (16), the state of health (SOH) degradation rate is derived, as illustrated in Figure 5. These relationships help us analyze the impact of current and environmental conditions on battery capacity and its overall health status.

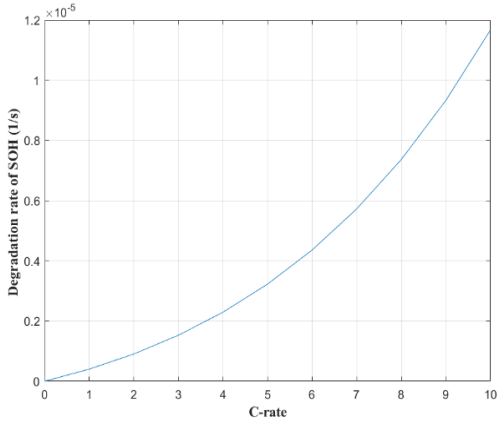

Figure 5: Battery health level decay rate as a function of current intensity

5. Energy management strategy in hybrid fuel cell vehicles

A fuzzy logic–based controller plays a central role in optimizing energy management for hybrid fuel cell vehicles. By enabling real-time decision-making, it regulates power flow between the fuel cell and supplementary energy storage units, thereby improving system efficiency and extending component durability. The controller evaluates two primary inputs battery SOC and instantaneous power demand to determine the appropriate power distribution strategy. In this study, five membership functions were designed for each input variable SOC and power demand—while seven membership functions were defined for the output variable. Figure 6 depicts the fuzzy membership functions alongside the corresponding fuzzy inference surface. The fuzzy control rules, summarized in Table 3, are grounded on the following principles:

- Under conditions of elevated power demand and diminished SOC, the fuel cell delivers the required power to sustain vehicle operation.
- When power requirements diminish and SOC levels rise, the battery becomes the primary source for meeting the vehicle's energy demands.

This rule-based fuzzy logic approach offers robustness and adaptability to varying driving conditions, ensuring smooth power transitions and efficient energy utilization. Through expert-driven fuzzy logic rules and membership functions, the controller achieves efficient load-sharing, minimizes fuel cell degradation, and extends the hybrid system's operational lifespan.

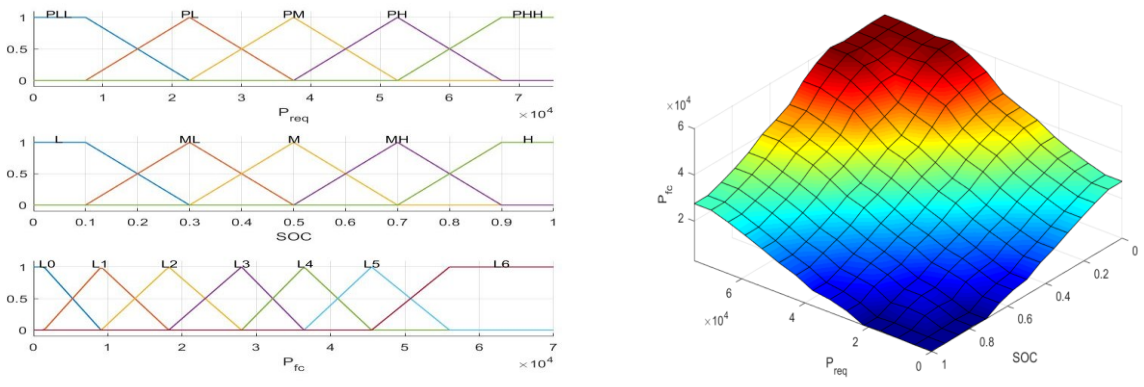

Figure 6: Input and output membership functions and fuzzy level for FCHEV

[Downloaded from ahc.iust.ac.ir on 2026-06-05]

[DOI: 10.22068/ase.2025.719]

Table 3: Rules based on fuzzy controllers

P_{req} / SOC	PLL	PL	PM	PH	PHH
L	L3	L4	L5	L6	L6
ML	L2	L3	L4	L5	L6
M	L1	L2	L3	L4	L5
MH	L0	L1	L2	L3	L4
H	L0	L0	L1	L2	L3

6. Optimizing energy management strategy with genetic algorithm

The fuzzy controller is optimized using a Genetic Algorithm (GA) to enhance performance. The GA adjusts the membership functions and fuzzy rules through selection, crossover, and mutation processes, conducting an extensive search across the parameter space to determine optimal values. As shown in Figure 7, the fuzzy logic EMS is optimized via a genetic algorithm that calculates fuel consumption and estimates fuel cell and battery longevity under the target driving conditions. A cost function is defined and executed at each iteration to achieve effective optimization, updating the fuzzy controller's parameters to minimize this cost[27].

The optimization leads to improved energy management, increased efficiency, reduced operational costs, and extended durability of the fuel cell system.

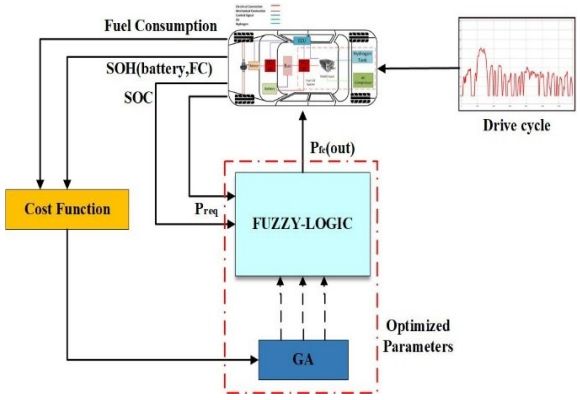

Figure 7: Schematic of fuzzy logic optimization using GA algorithms

The optimization of the fuzzy controller in this study pursues two key objectives:

1. **Fuel Consumption Reduction:** Minimizing hydrogen consumption in the fuel cell enhances efficiency and reduces operational costs.

2. **Extension of Battery and System Lifespan:** Implementing intelligent energy management strategies to reduce operational stress on critical components, including the fuel cells and batteries, increases system durability.

To ensure the simultaneous fulfillment of these critical requirements, the objective function is defined as follows:

$$\min J = w_{h_2} M_{H_2} + w_{fc} R_{SOH} + w_{bat} B_{SOH} \quad (17)$$

The term B_{SOH} represents the battery degradation, where M_{H_2} denotes the hydrogen consumption rate and R_{SOH} indicates the cost of fuel cell degradation due to the collapse of the ECSA, assuming a 75% loss at the end-of-life of the fuel cell stack. Additionally, w_{h_2}, w_{fc}, and w_{bat} represent the weights of the hydrogen consumption rate, the cost of fuel cell and battery degradation, respectively. The objective function simultaneously reduces fuel consumption and increases system lifespan, prioritizing battery SOC as a critical constraint. This enables the controller to optimize performance and durability via adaptive, constraint-focused strategies. The GA optimization required approximately 28s per tuning run on an 8-core workstation; deployments use only the tuned rule base, so online control remains lightweight.

6.1. Constraints

The battery's SOC must be rigorously constrained during energy management optimization to prevent deep discharge and overcharging, which degrade battery health

[Downloaded from ahc.iust.ac.ir on 2026-06-05]

[DOI: 10.22068/ase.2025.719]

and reduce overall system performance. Optimal system performance requires maintaining the battery's state of charge within a specified operational window as follows:

$$SOC_{min} < SOC(t) < SOC_{max} \quad (18)$$

To safeguard battery health, SOC_{min} is fixed at 0.4 to prevent excessive discharge, and SOC_{max} is restricted to 0.8 to minimize electrochemical strain and degradation. Additionally, to prevent sudden fluctuations and reduce battery stress, the rate of change of SOC must be controlled:

$$\Delta SOC_{max} \geq \left|\frac{SOC_{k+1}-SOC_k}{dt}\right| \quad (19)$$

This constraint guarantees that variations in the SOC happen smoothly and are controlled, minimizing stress on the battery. Figures 8 and 9 below illustrate the outcomes of the genetic algorithm optimization applied to the fuzzy controller, evaluated across the UDDS and Tehran driving cycles.

The GA optimization was carried out offline during the design phase to determine the optimal fuzzy rule parameters. Although the optimization process is computationally demanding, it is executed only once prior to implementation. During dynamic simulation, the optimized FLC operated smoothly and stably without noticeable computational lag, confirming the practicality of the proposed GA–FLC framework for future embedded applications.

6.2. Robustness Verification under Noisy Driving Conditions

To further evaluate robustness, a modified driving cycle was generated by introducing slight slope variations and stochastic noise into the vehicle power-demand profile. The optimized GA–FLC controller maintained stable operation and consistent convergence behavior under these fluctuating conditions, confirming reliable optimization performance. Although the GA parameters (population = 40, generations = 20) were kept fixed, five independent runs using different random seeds showed less than 4% variation in the final fitness value and maintained at least five distinct fuzzy rule sets at convergence. This demonstrates that the controller exhibits stable convergence, adequate population diversity, and resilience against noisy driving scenarios.

7. Results

Simulations of the fuel cell hybrid vehicle's dynamic behavior under UDDS and Tehran driving cycles were conducted to validate the GA-optimized energy management strategy, specifically examining its influence on fuel cell power output and battery SOC to prolong component durability.

As illustrated in Figure 10, GA-based optimization significantly reduces power fluctuations in the fuel cell, resulting in smoother and more stable operation. In contrast, the non-optimized system exhibits rapid and pronounced power variations, increasing electrochemical and thermal stresses. A more uniform load distribution achieved through optimization is essential for enhancing fuel cell durability. Similarly, Figure 11 demonstrates that the GA-optimized strategy maintains a higher battery SOC with more controlled discharge behavior. Minimizing deep discharges and improving SOC recovery, the battery experiences reduced degradation, improving overall system stability.

Figure 12 further reveals that although the optimized system experiences more frequent power fluctuations during the initial phases of operation, the amplitude of these fluctuations is significantly lower, leading to smoother

[Downloaded from ahc.iust.ac.ir on 2026-06-05]

[DOI: 10.22068/ase.2025.719]

transitions. Conversely, the non-optimized system undergoes sharp and abrupt power changes, particularly during the early and mid stages of the cycle, imposing severe electrochemical, thermal, and mechanical stresses on the fuel cell.

These stresses accelerate structural degradation. In contrast, the optimized system achieves a more gradual and consistent power output profile, promoting enhanced stability. In Figure 13, the battery SOC rises, indicating energy input from the fuel cell or regenerative braking mechanisms. After reaching a peak of approximately 0.76, the SOC gradually decreases as the battery delivers energy. The SOC returns close to its initial value, by the end of the driving cycle, evidencing effective energy management and balanced charge maintenance.

The results from the Tehran driving cycle highlight that GA-based optimization can significantly mitigate damaging stresses and improve the durability of key vehicle components by achieving smoother fuel cell loading and optimized battery SOC management. Critically, enhancing fuel cell lifespan depends on minimizing the frequency of load fluctuations and controlling the intensity, amplitude, and slope of load variations throughout vehicle operation.

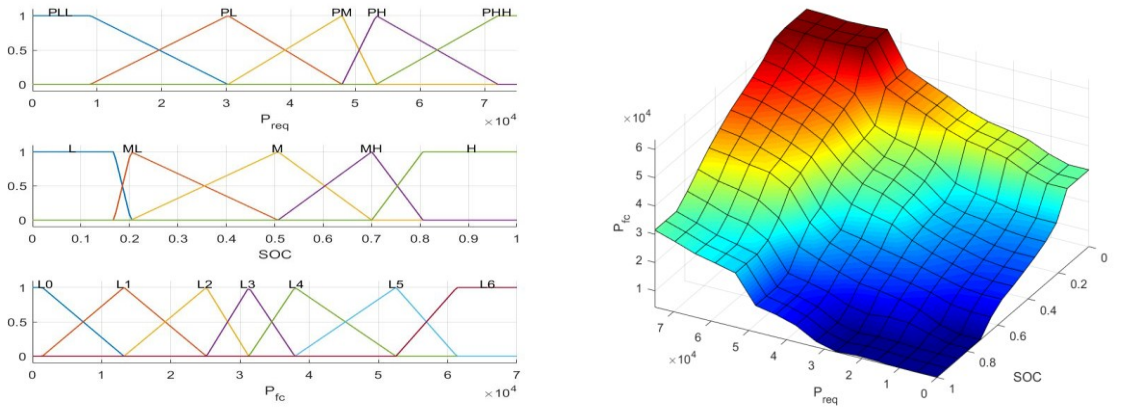

Figure 8: Schematic of fuzzy logic optimization using GA algorithms UDDS drive cycle

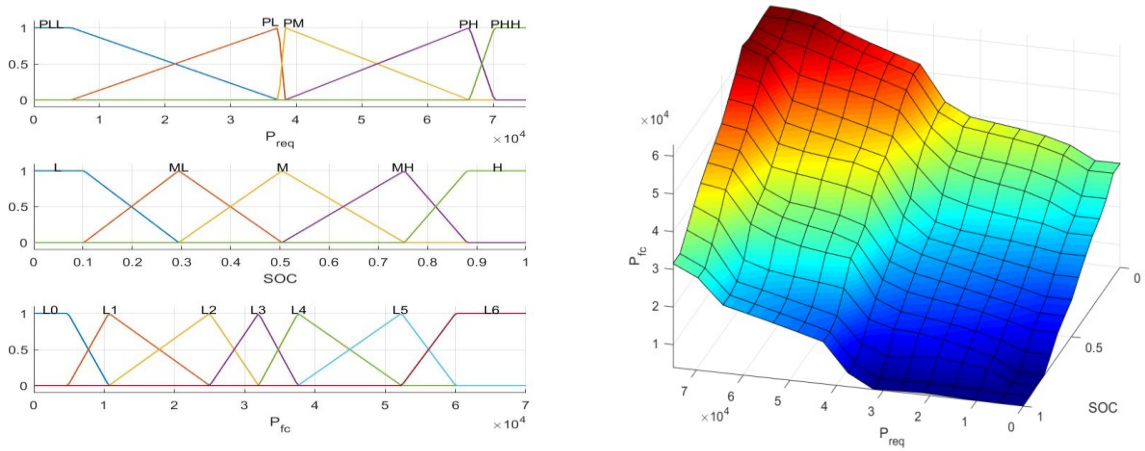

Figure 9: Schematic of fuzzy logic optimization using GA algorithms TEHRAN drive cycle

[Downloaded from ahc.iust.ac.ir on 2026-06-05]

[DOI: 10.22068/ase.2025.719]

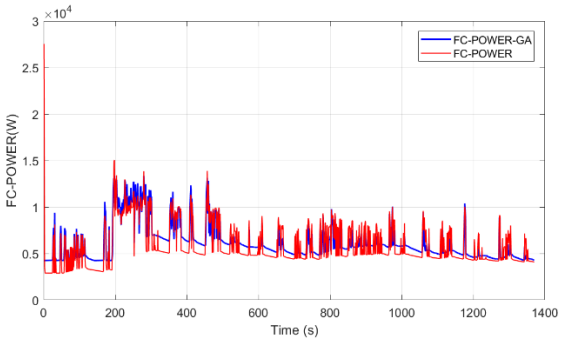

Figure 10: Fuel cell power (UDDS drive cycle)

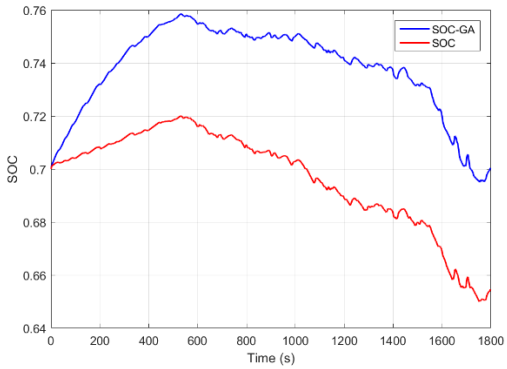

Figure 13: battery state of charge (TEHRAN drive cycle)

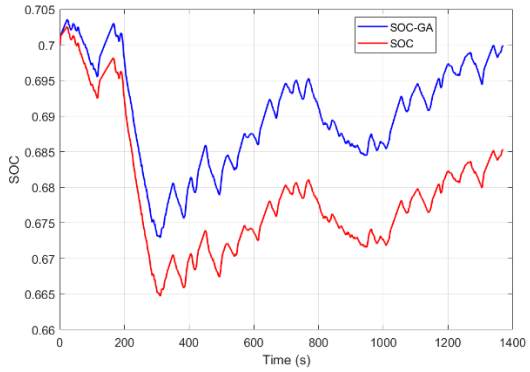

Figure 11: battery state of charge (UDDS drive cycle)

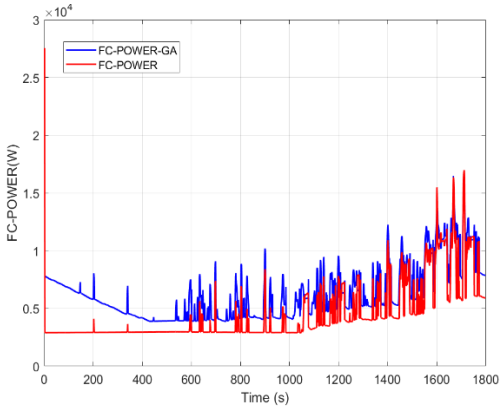

Figure 12: Fuel cell power (TEHRAN drive cycle)

Simulation results under various driving cycles, including UDDS and Tehran, demonstrated the superiority of the optimized approach compared to baseline strategies. According to the data presented in Table 4, employing a GA for optimizing the fuzzy controller significantly reduced fluctuations in the fuel cell output power—one of the main contributors to the accelerated degradation of this costly component. This reduction directly translated into an extended estimated system lifespan, with improvements of approximately 50.6% and 12.9% observed under the Tehran and UDDS driving cycles, respectively. Furthermore, a detailed battery aging analysis revealed that the optimized strategy substantially decreased the lithium-ion battery capacity fade rate, ensuring its long-term health. Overall, GA-based optimization increased the system's longevity, reduced battery degradation, enhanced the state of charge stability, and improved overall energy management efficiency. In the proposed control strategy, regenerative braking was also considered during the simulation. The recovered braking energy was fully routed to the Li-ion battery through the energy management controller, enabling partial recovery of kinetic energy that would otherwise be dissipated as heat. Consequently, hydrogen consumption decreased by

[Downloaded from ahc.iust.ac.ir on 2026-06-05]

[DOI: 10.22068/ase.2025.719]

approximately 7.8%, while the battery experienced a modest 3.4% increase in charge–discharge cycling depth. This represents a trade-off between enhanced overall energy efficiency and slightly higher battery utilization under regenerative-braking conditions. The same degradation model can be readily re-parameterized for other battery chemistries—such as LFP or NMC—by adjusting the activation-energy and depth-of-discharge exponents, ensuring that the proposed GA-FLC strategy remains applicable across diverse hybrid configurations. As shown in Table 4, the equivalent fuel needed to restore the final SOC to its initial level in the non-optimized case is roughly equal to the optimized fuel use for reaching the same charge state. The equivalent fuel is estimated by converting the net battery energy difference (between final and initial SOC) into an equal amount of hydrogen, using the fuel cell's average efficiency and hydrogen's lower heating value. This highlights the importance of balancing fuel use and battery performance to improve efficiency and extend fuel cell life.

Table 4: Optimized and non-optimized results under driving cycles

	TEH		UDDS	
Result	None-opt	GA	None-opt	GA
Hydrogen Consumption (g/100km)	779.37	937.21	745.68	782.24
Lifetime(h)	1412	2127	1943	2195
Capacity loss Battery (%)	0.009	0.0081	0.0081	0.0077
SOC_{int}	0.7	0.7	0.7	0.7
SOC_{final}	0.634	0.7	0.685	0.7
Hydrogen Equivalent Consumption (g/100km)	971.32	937.21	794.41	782.24

8. Conclusions

This research aimed to address the critical challenge of enhancing the durability of fuel cells and batteries in FCHEVs under realistic operating conditions. A significant step was taken by presenting a comprehensive framework that included detailed dynamic modeling of the vehicle, analysis of the degradation mechanisms of key components (specifically platinum dissolution in PEMFCs and the impact of SOC, current rate, and temperature on Lithium-ion battery aging), and optimization of the energy management strategy—implementing degradation models based on physical principles and experimental data allowed for accurate assessment of the state of health and prediction of the lifespan of these components.

The developed fuzzy logic controller-based energy management strategy, optimized using a Genetic Algorithm, demonstrated high reliability in allocating power between the fuel cell and battery across diverse driving cycles, including the standard UDDS cycle and the realistic Tehran traffic cycle. Simulation results proved the effectiveness of the optimized approach in reducing fuel cell power fluctuations, a significant factor in accelerating its degradation. Furthermore, this strategy led to a considerable improvement in the estimated lifespan of the overall hybrid system; we observed an approximate increase of 50.6% and 12.9% in lifespan for the Tehran and UDDS cycles, respectively, compared to the baseline strategy. The notable reduction in the Lithium-ion battery capacity fade rate per cycle traversal (e.g., a decrease from 0.009% to 0.0081% for the Tehran cycle) highlights another advantage of this method in preserving

[Downloaded from ahc.iust.ac.ir on 2026-06-05]

[DOI: 10.22068/ase.2025.719]

battery health and postponing its end-of-life point. In addition to improved durability, the optimized strategy reduced equivalent fuel consumption while maintaining the battery's state of charge within the optimal operating range, indicating higher efficiency of the energy management system. In conclusion, this study showed that integrating accurate component degradation models with advanced energy management optimization offers a powerful approach to designing FCHEVs with higher durability and efficiency. The findings of this research contribute to a better understanding of degradation dynamics under real-world driving conditions and provide practical solutions for extending the lifespan and reducing the operational costs of FCHEVs, thereby paving the way for broader adoption of these clean and sustainable vehicles in the future. Future work will focus on implementing the GA–FLC controller in a hardware-in-the-loop (HIL) setup using Speedgoat and real PEMFC–battery modules. This experiment will enable evaluation of real-time adaptability under stochastic thermal and traffic variations. The proposed GA-FLC strategy achieved simultaneous improvements in durability and efficiency under standardized and real-world cycles. Future research will incorporate adaptive scheduling of membership functions based on temperature and traffic variability, along with probabilistic validation over diverse urban driving datasets, to reinforce robustness and real-time applicability.

List of symbols (Optional)

$\bar{I}_c$	Avrage current rate
E_a	Activation energy
E_{Gt}	Gibbs-Thomson energy (J/mol)
E_{rev}	reversible voltage (V)
F	Faraday constant (c/mol)
$\bar{I}_c$	Avrage current rate
i	current density (A/ cm²)
i_{loss}	decrease in crossover current density (A/cm^2)
$i_{loss,o}$	intital loss current density (A/ cm²)
$i_{loss,1}$	decay rate of loss current density(1/h)
$i_{o,a}$	Exchange current density at the anode (A/ cm²)
$i_{o,c}$	Exchange current density at the cathode (A/ cm²)
k	direct reaction constant (mol/$m^2.s$)
M_{pt}	molar mass (kg/mol)
m_t	concentration loss (V)
m_0	Initial parameter of m_t (V)
m_1	Aging parameter of m_t (1/h)
n_t	concentration loss (cm²/A)
n_0	Initial parameter of n_t (cm²/A)
n_1	Aging parameter of n_t (1/h)
PtO	platinum oxide
Q_{loss}	Normalized capacity loss (%)
Q_{bat}	battery capacity (Ah)
R	gas constant (J/K.kg)
R	ohmic resistance (ohm.cm²)
R_0	initial resistance (ohm/ cm²)
R_1	growth rate of resistance (1/h)
r_{pt}	radius of platinum (m)

[Downloaded from ahc.iust.ac.ir on 2026-06-05]

[DOI: 10.22068/ase.2025.719]

T, θ	Temperature (K)
i_{loss}	decrease in crossover current density (A/cm^2)
R_{ohm}	ohmic resistance (ohm. cm^2)
m_t	concentration loss (V)
n_t	concentration loss (cm^2/A)
V	Voltage (V)
V_{ocv}	open circuit voltage (V)
V_{pto}	decrease platinum voltage (V)
$V_{pto,1}$	Aging parameter of V_{pto} (1/h)
$V_{pto,o}$	Initial parameter of V_{pto} (V)
z	Power low exponent

Greek symbols

α, β	Model parameters
α_k	reaction transfer coefficient (-)
β	transfer coefficients (-)
ΔG_s	free energy of platinum extraction (J)
ΔG_{elec}	free energy of oxidation (J)
ΔG_{des}	free energy of desorption (J)
ΔSOC	Rate of change of state of charge
$\Delta\chi$	local potential (V)
γ_{pt}	surface energy of platinum (J/m^2)
ρ_{pt}	density (kg/m^3)
σ_{func}	Severity factor function
v_{diss}	kinetic dissolution rate of platinum (m/s)

References

[1] S. F. Da Silva *et al.*, "Aging-aware optimal power management control and component sizing of a fuel cell hybrid electric vehicle powertrain," *Energy Convers. Manag.*, vol. 292, p. 117330, Sep. 2023, doi: 10.1016/j.enconman.2023.117330.

[2] R. Ghaderi, M. Kandidayeni, M. Soleymani, and L. Boulon, "Investigation of the Battery Degradation Impact on the Energy Management of a Fuel Cell Hybrid Electric Vehicle," in *2019 IEEE Vehicle Power and Propulsion Conference (VPPC)*, Hanoi, Vietnam: IEEE, Oct. 2019, pp. 1–6. doi: 10.1109/VPPC46532.2019.8952303.

[3] H. Li, H. Chaoui, and H. Gualous, "Cost Minimization Strategy for Fuel Cell Hybrid Electric Vehicles Considering Power Sources Degradation," *IEEE Trans. Veh. Technol.*, vol. 69, no. 11, pp. 12832–12842, Nov. 2020, doi: 10.1109/TVT.2020.3031000.

[4] C. Liu and L. Liu, "Optimal power source sizing of fuel cell hybrid vehicles based on Pontryagin's minimum principle," *Int. J. Hydrog. Energy*, vol. 40, no. 26, pp. 8454–8464, Jul. 2015, doi: 10.1016/j.ijhydene.2015.04.112.

[5] H. Kim, T. Jung, J. Jung, Y. Noh, and B. Lee, "Accurate Prediction of Electrochemical Degradation Trajectory for Lithium-Ion Battery Using Self-Discharge," *Int. J. Energy Res.*, vol. 2024, no. 1, p. 1758578, Jan. 2024, doi: 10.1155/2024/1758578.

[6] C. Lin, W. Luo, H. Lan, and C. Hu, "Research on Multi-Objective Compound Energy Management Strategy Based on Fuzzy Control for FCHEV," *Energies*, vol. 15, no. 5, p. 1721, Feb. 2022, doi: 10.3390/en15051721.

[7] B. Geng, J. K. Mills, and D. Sun, "Combined power management/design optimization for a fuel cell/battery plug-in hybrid electric vehicle using multi-objective particle swarm optimization," *Int. J. Automot. Technol.*, vol. 15, no. 4, pp. 645–654, Jun. 2014, doi: 10.1007/s12239-014-0067-x.

[8] B. Geng, J. K. Mills, and D. Sun, "Two-Stage Energy Management Control of Fuel Cell Plug-In Hybrid Electric Vehicles Considering Fuel Cell Longevity," *IEEE Trans. Veh. Technol.*, vol. 61, no. 2, pp. 498–508, Feb. 2012, doi: 10.1109/TVT.2011.2177483.

[9] T. Fletcher and K. Ebrahimi, "The Effect of Fuel Cell and Battery Size on Efficiency and Cell Lifetime for an L7e Fuel Cell Hybrid Vehicle," *Energies*, vol. 13, no. 22, p. 5889, Nov. 2020, doi: 10.3390/en13225889.

[10] M. Montazeri-Gh and E. Alimohammadi, "Online battery aging calculation in plug-in hybrid electric vehicle considering driving condition," *Energy Sources Part Recovery Util. Environ. Eff.*, vol. 46, no. 1, pp. 5324–5343, Dec. 2024, doi: 10.1080/15567036.2024.2338870.

[11] M. Masih-Tehrani, M.-R. Ha'iri-Yazdi, V. Esfahanian, and A. Safaei, "Optimum sizing and optimum energy management of a hybrid energy storage system for lithium battery life improvement," *J. Power Sources*, vol. 244, pp. 2–10, Dec. 2013, doi: 10.1016/j.jpowsour.2013.04.154.

[12] J. Li, X. Wu, M. Xu, and Y. Liu, "A real-time optimization energy management of range extended electric vehicles for battery lifetime and energy consumption," *Journal of Power Sources*,

[Downloaded from ahc.iust.ac.ir on 2026-06-05]

[DOI: 10.22068/ase.2025.719]

vol. 498, p. 229939, Jun. 2021. https://doi.org/10.1016/j.jpowsour.2021.229939

[13] C. Robin, M. Gérard, M. Quinaud, J. d'Arbigny, and Y. Bultel, "Proton exchange membrane fuel cell model for aging predictions: Simulated equivalent active surface area loss and comparisons with durability tests," *Journal of Power Sources*, vol. 326, pp. 417–427, Sep. 2016. https://doi.org/10.1016/j.jpowsour.2016.07.018

[14] M. Gerard, C. Robin, M. Chandesris, and P. Schott, "(Invited) Polymer Electrolyte Fuel Cells Lifetime Prediction By a Full Multi-Scale Modeling Approach," *ECS Trans.*, vol. 75, no. 14, pp. 35–43, Aug. 2016. https://doi.org/10.1149/07514.0035ecst

[15] V. A. Sarbast, "Modeling of Proton Exchange Membrane Fuel Cell Performance Degradation and Operation Life".

[16] R. Mukundan *et al.*, "Membrane Accelerated Stress Test Development for Polymer Electrolyte Fuel Cell Durability Validated Using Field and Drive Cycle Testing," *J. Electrochem. Soc.*, vol. 165, no. 6, pp. F3085–F3093, 2018. https://doi.org/10.1149/2.0101806jes

[17] T.-C. Jao, G.-B. Jung, S.-C. Kuo, W.-J. Tzeng, and A. Su, "Degradation mechanism study of PTFE/Nafion membrane in MEA utilizing an accelerated degradation technique," *International Journal of Hydrogen Energy*, vol. 37, no. 18, pp. 13623–13630, Sep. 2012. https://doi.org/10.1016/j.ijhydene.2012.02.035

[18] L. Mao, L. Jackson, and T. Jackson, "Investigation of polymer electrolyte membrane fuel cell internal behaviour during long term operation and its use in prognostics," *Journal of Power Sources*, vol. 362, pp. 39–49, Sep. 2017. https://doi.org/10.1016/j.jpowsour.2017.07.018

[19] J. Han, J. Han, and S. Yu, "Investigation of FCVs durability under driving cycles using a model-based approach," *Journal of Energy Storage*, vol. 27, p. 101169, Feb. 2020. https://doi.org/10.1016/j.est.2019.101169

[20] M. J. Esfandyari, M. R. Hairi Yazdi, V. Esfahanian, M. Masih-Tehrani, H. Nehzati, and O. Shekoofa, "A hybrid model predictive and fuzzy logic based control method for state of power estimation of series-connected Lithium-ion batteries in HEVs," *J. Energy Storage*, vol. 24, p. 100758, Aug. 2019, doi: 10.1016/j.est.2019.100758.

[21] Wang J, Liu P, Hicks-Garner J, Sherman E, Soukiazian S, Verbrugge M, et al. Cycle-life model for graphite-LiFePO4 cells. J Power Sources 2011;196:3942e8.

[22] F. Todeschini, S. Onori, G. Rizzoni, An experimentally validated capacity degradation model for Li-ion batteries in phev applications, 8th IFAC International Symposium on fault detection, Supervision and Safety of technical processes.

[23] Omar N, Monem MA, Firouz Y, Salmien J, Smekens J, Hagazy O, et al. Lithium iron phosphate based battery - assessment of aging parameters and development of life cycle model. Appl Energy 2014;113:1575e85

[24] Serrao L, Onori S, Rizzoni G, Guezennec Y. A novel model-based algorithm for battery prognosis. In: Proceeding of the 7th IFAC Symposium on fault detection, Supervision and Safety of technical processes. Barcelona: Spain; 2009. [10] K. Steffke, S. Inguva, D. Cleve, Knockeart J., Accelerated life test methodology for Li-ion batteries in automotive applications

[25] A. Ansari Laleh and M. H. shojaeefard, "A Comprehensive Review of Phase Change Materials and Their Application in Thermal Management Systems of Lithium-ion Batteries," *Automot. Sci. Eng.*, vol. 14, no. 4, Dec. 2024, doi: 10.22068/ase.2024.695

[26] G. Suri and S. Onori, "A control-oriented cycle life model for hybrid electric vehicle lithium-ion batteries," Energy, vol. 96, pp. 644–653, Feb. 2016, doi: 10.1016/j.energy.2015.11.075.

[27] M. H. Alsulami et al., "Hybrid genetic algorithm and linear programming for emissions and fuel-consumption management using continuously variable transmission," *Journal of Construction Engineering and Management*, vol. 144, no. 2, 2018, doi: 10.1061/(ASCE)CO.1943-7862.0001490.

[Downloaded from ahc.iust.ac.ir on 2026-06-05]

[DOI: 10.22068/ase.2025.719]